



Amoeboid Movement Anchored by Eupodia, New Actin-Rich Knobby Feet in *Dictyostelium*

Yoshio Fukui^{1*} and Shinya Inoué²

¹*Cell and Molecular Biology, Northwestern University Medical School, Chicago, Illinois*

²*Marine Biological Laboratory, Woods Hole, Massachusetts*

To date, protrusion of pseudopodia has been considered to be primarily responsible for translocation of free-living amoebae and leukocytes of higher organisms. Although there is little question that the pseudopodium plays an important role, little attention has been given to the cortical structures that are responsible for cell-substratum anchorage in amoeboid movement. Here, we report on a new knobby foot-like structure in amoebae of a cellular slime mold, *Dictyostelium discoideum*. These feet, each about 1 μm in diameter, appear transiently in multiple units at the base of certain pseudopodia where the amoeba contacts a partially deformable substrate. The feet were discovered, and their spatial and temporal behavior relative to pseudopodial anchorage and invasive locomotion were observed, by examining *Dictyostelium* amoebae using a DIC video microscope providing an 0.3 μm depth of field. Key evidence for the anchoring role of the knobby feet was obtained by investigating amoebae, flattened in a specially devised observation chamber, and attracted by chemotaxis towards 3',5' cyclic-adenosine monophosphate (cAMP). The cAMP was released by highly localized, pulsed UV-microbeam irradiation of caged cAMP. We show by indirect immunofluorescence that the knobby feet contain a high concentration of filamentous (F-) actin, myoB (a member of *Dictyostelium* myosin-I family), and α -actinin (an actin-binding protein). Interestingly, myoB exhibits a circular disposition around each foot. Neither myosin-II (conventional myosin) nor the 269 kD protein, which has been recently identified as a talin homologue of *Dictyostelium* [Kreitmeier et al., 1995: *J. Cell Biol.* 129:179–188], are concentrated at the feet. We propose that the knobby feet provide anchorage to the substratum needed by lamellipodia to exert projectile forces for invading narrow spaces or otherwise for a flattened amoeba to secure itself to the deformable substratum. Some forms of adhesion plaques in higher organisms such as “podosomes” or “invadopodia” may perform functions similar to the knobby feet, but appear to differ in life time, cytoskeletal organization and composition. We have named the knobby foot “eupodium.” *Cell Motil. Cytoskeleton* 36:339–354, 1997. © 1997 Wiley-Liss, Inc.

Key words: caged cAMP; chemotaxis; pseudopodia; ultrathin optical section; UV microbeam

INTRODUCTION

The term, pseudopodium refers to motile protrusive structures such as lobopodia (broad, thick protrusions found in amoeboid cells), filopodia (slender, finger-like projections found in a wide variety cells), axopodia (radial array of thin, long protrusions of *Heliozoa*), and myxopodia or rhizopodia (anastomosing cytoplasmic networks of *Myxomycetes* and *Rhizopoda*) [Hartmann, 1953]. Thin, veil-like protrusions formed by tissue cul-

Video tape documenting these observations has been accepted to be incorporated into a video supplement.

Contract grant sponsor: NIH; Contract grant numbers: ROI-GM39548 and R37-GM31617.

*Correspondence to: Dr. Yoshio Fukui, CMB, Northwestern Medical School, Ward 8-132, 303 East Chicago Avenue, Chicago, IL 60611-3008. E-mail: yoshifk@casbah.acns.nwu.edu

Received 17 July 1996; accepted 11 November 1996.

ture cells exhibiting ruffling movement (lamellipodia) are also classified as pseudopodium [Abercrombie et al., 1971]. All these are transient, actin-supported structures except axopodia and myxopodia, which are microtubule-supported semi-permanent (though rapidly contractile) structures.

Since Dejardin [1835], *Amoeba proteus* has served as a paradigm for studying the mechanism of amoeboid movement. The classic literature focused primarily on cytoplasmic streaming and gel-sol transformation and did not address the significance of amoeba-substrate attachment [Hyman, 1917; Mast, 1923; Pantin, 1923; review, Fukui and Yumura, 1986]. Nevertheless, it should be noted that Mast [1926], and earlier Dellinger [1906] in a most interesting paper, described an intriguing observation from the side of the amoeba in which they suggested the role played by a downward branch of the anterior pseudopodium towards the substratum in the crawling translocation of the amoeba. These workers interpreted the local contact of the anterior extension to the substratum as a means for supporting the buoyant weight, and providing a pivot for a forward tumbling by the giant amoebae that they were studying.

More than 20 years ago, Taylor et al. [1973] demonstrated that amoeboid streaming occurs in demembrated *A. proteus*. In that study, they implicated an important role of attachment of plasma membrane, along with glycocalyx, to the substratum for amoeboid locomotion. More recently, Grebecki [1984, 1986] indicated the occurrence of a direct connection between the adhesion sites and the cytoskeleton in *A. proteus* based on detailed video microscopic analysis [review: Grebecki, 1994]. However, amazingly little is known about the structure, dynamics, and components of the attachment sites in such amoeboid cells as *A. proteus*, *Dictyostelium discoideum*, and leukocytes.

In tissue cultured cells, adhesion plaques were first identified as focal points formed along stress fibers in slowly moving cells such as fibroblasts and epithelial cells [Abercrombie et al., 1971]. They are 2–10 μm long, 0.25–0.5 μm wide structures which are believed to play crucial role in anchoring the stress fibers to the substratum [review; Burridge et al., 1988]. Adhesion plaques are only formed by cells cultured on a solid substratum but not by fibroblasts grown in collagen gels where the cells do not form discernible stress fibers [review; Burridge et al., 1988]. It is known that there is a sophisticated mechanical linkage and signal transduction network in the adhesion plaques involving proteins such as F-actin, α -actinin, vimentin, talin, α , β -integrins, and fibronectin (or vitronectin). The role of talin has been an issue of controversy because of its weak interaction with vinculin, which connects talin to F-actin [review Turner and Burridge, 1991].

Podosomes are dot-shaped sites of cell-substrate adhesion originally found in fibroblasts transformed by Rous sarcoma virus (RSV) [Tarone et al., 1985; Nermut et al., 1991], and more recently also called invadopodia [Mueller et al., 1992]. They are similar to adhesion plaques in composition but differ in several aspects including speed of formation (i.e., they appear in the initial 60 min of attachment while normal adhesion plaques require at least 180 min), and structure (i.e., podosomes are formed independent of stress fibers) [review Burridge et al., 1988]. Podosome-like structures are also formed by normal blood cells when they are penetrating the narrow space between endothelial cells [Wolosewick, 1984], or by osteoclasts during calcium resorption [Lakkakorpi and Väänänen, 1991]. In short, podosomes appear to be invasive protrusions formed from the ventral surface toward the substrate, and are considered to be a phenotypic variant of adhesion plaques [Tarone et al., 1985].

In *D. discoideum*, filopodia, lamellipodia, and lobopodia have been the only reported cortical structures so far believed to be involved in amoeboid locomotion. We report here that *Dictyostelium* amoeba also form foot-like, knobby cortical protrusions, in a reversible and dynamic manner, when it appears to require a firm anchorage to the substratum. To demonstrate that these cortical protrusions provide anchorage for invasive pseudopodial extension, we devised a new observation chamber and a method for attracting amoebae into thin spaces by highly localized, controlled release of cAMP using UV-microbeam uncaging of “caged” cAMP.

In the following we also show that the knobby cortical protrusions contain a high concentration of F-actin, α -actinin, and myosin-I, but not talin. In several aspects, this structure is different from adhesion plaques and related structures. Based on its structure and function, we name this structure “*eupodium*” (Gr., *eu* = true, primitive, *podos* = foot) as contrasted to “*pseudopodium*.” A preliminary account of this structure appears in Fukui and Inoué (Biol. Bull., Oct., 1995) and Inoué and Fukui (Mol. Biol. Cell, 6, 261a, 1995).

MATERIALS AND METHODS

Cells and Cultures

Wild type amoebae (strain A x 3) of *D. discoideum* were cultured in a plastic flask with a 25 cm² bottom area (Falcon 3013; Becton Dickinson Labware, NY) containing 4.5 ml of HL5 medium made of proteose peptone, yeast extract, D-glucose, and Na/K-PO₄ (pH 6.5) [Cocucci and Sussman, 1970]. At late exponential phase, the medium was replaced with Bonner's salt solution containing 10 mM NaCl, 10 mM KCl, and 3 mM CaCl₂ [Bonner, 1947]. The cells were incubated for 2–3 h at 22°C, and stationary stage amoebae were scraped off from the

bottom of the flask with a silicone rubber policeman. Aggregation stage amoebae were prepared by incubating a confluent culture in Bonner's solution for 18 h at 18°C before scraping off. The scraping does not adversely affect the viability, motility, or chemotaxis of the amoebae.

Observation Chamber

2.25% agarose-M (LKB Produkter, Bromma, Sweden) was dissolved in Bonner's salt solution and allowed to gel between two pieces of clean microscope slides supported with 50 μm -thick spacers. A small piece of the agarose film (50 μm -thick, 5 x 5 mm^2) was cut out and placed in the middle of a 22 x 22 mm^2 glass coverslip (no. 1½, 170 μm -thick; Corning Glass Works, Corning, NY) before applying the cells. A 1 μl aliquot of cell suspension containing about 200 amoebae was spread over the surface of the agarose film and excess fluid was sucked off with a tiny wedge of filter paper. For experiments involving UV-microbeam uncaging of caged cAMP (c^2AMP ; see below), the agarose was pre-saturated with 100 mM c^2AMP . The sample overlaid with the cells was turned over and placed on a 22 x 40 mm^2 glass coverslip (no. 1½, 170 μm -thick) supported by a ring-shaped 50 μm -thick spacer made of Mylar 200D plastic film (Du Pont, Wilmington, PA) and sealed with VALAB (a 1:1:1 mixture of vaselline, lanolin, and bee's wax). The air space between the agarose and the opening in the Mylar spacer provided adequate oxygen supply for the amoebae to continue to divide for more than a day. This chamber design provided good viability of the flattened amoebae as well as the optical conditions needed for high resolution DIC and UV imaging. The sample was then attached to an aluminum holder with dental tacky wax (Fig. 1b).

Video Microscopy

For visual-light observation and recording, the specimen was imaged through a universal inverted polarizing microscope [Inoué, 1986] illuminated through a quartz fiber optic light scrambler with 546-nm monochromatic light. The microscope was equipped with a rectified, 1.4 NA oil immersion DIC condenser (Nikon Inc., Melville, NY) and a 60x or 100x, 1.4 NA plan apo oil immersion objective lens (Nikon, Inc.) with DIC optics (Fig. 1a). The images were captured with a compact CCD camera (see below). Under this condition, the x-y and z-axis resolutions were 0.2 μm and 0.3 μm respectively [Inoué, 1988], and the temporal resolution was 16.5 milliseconds per video field.

UV Microbeam Irradiation

An auxiliary UV illuminator was attached to the universal polarizing microscope for controlled release of cAMP from the caged compound (Fig. 1a). The amoebae were placed in an observation chamber (Fig. 1b) on the 5 x 5 mm^2 agarose film saturated with 100 μM cAMP

[Nerbonne et al., 1984] dissolved with 5 mM Hepes (pH 6.7) in Bonner's salt solution. The microscope system was modified from Inoué [Fig. III-21, 1986] in a manner similar to that described in Walker et al. [1989]. The modification includes the use of a mercury-Xenon arc lamp (model HPK L2422-01; Hamamatsu Photonics Systems, Bridgewater, NJ) as the visible light source, and replacement of the condenser with a glycerol-immersion, UV-transmitting objective lens (Ultrafluor 100x, NA 1.25; Carl Zeiss, Inc.) equipped with a DIC prism. A high-pressure HBO 100W mercury arc with quartz collector lens attached to a side rail of the microscope was used as the auxiliary UV source. The lamp output was filtered through a 366-nm band-pass filter (a combination of a Corning or Edmund Scientific [Barrington, NJ] heat cut filter that removes wavelength below 350 nm and a UG2 fluorescence excitation filter that removes wavelength above 380 nm). The UV beam, controlled with an electronic shutter (UniBlitz model D122; Vincent Associates, Rochester, NY), was reflected from a first-surface micromirror (0.15 x 0.35 mm^2 or 0.15 x 0.25 mm^2) placed in front of the field stop (Fig. 1a). The micromirror was positioned about 175 mm (instead of the standard projection distance of 150 mm) from the shoulder of the Ultrafluor lens used in place of a condenser. With this setting, the 60x or 100x plan apo objective provided a good UV image (e.g., Fig. 5b) of the micromirror through the 170 μm -thick glass coverslip and 50 μm -thick agarose (see above). The CCD camera had adequate sensitivity to capture the 546 nm green DIC image together with the image of the intense ultraviolet microbeam even after attenuation. To prevent excess UV light from entering the CCD camera, a "UV cut-off" filter (LL400-F-N963; Corion Corp., Holliston, MA) was inserted between the zoom ocular and the camera. The microbeam was delivered as a series of 3 or 30 msec flashes repeated every 650 msec.

The cells exposed to the intense 546 nm green light had to be kept at a room temperature no warmer than 21°C. At that temperature, we continuously observed healthy cells undergoing amoeboid movement for many hours, whether or not the amoebae were exposed to the c^2AMP -uncaging UV flashes. At room temperature of 23°C, the amoebae rounded up and stopped pseudopodia formation in several minutes under 546-nm green monochromatic illumination alone.

Imaging Technique

Images of living cells were recorded onto video tape using a Sony Extended Definition (ED)-Beta VCR and a Sony optical memory disk recorder (Sony Corp., USA, Paramus, NJ) in real time through a Hamamatsu Photonics Systems' model C-2400 CCD video camera. The image was processed with an Image-1/AT Digital Imaging Processor (Universal Imaging Corp., West

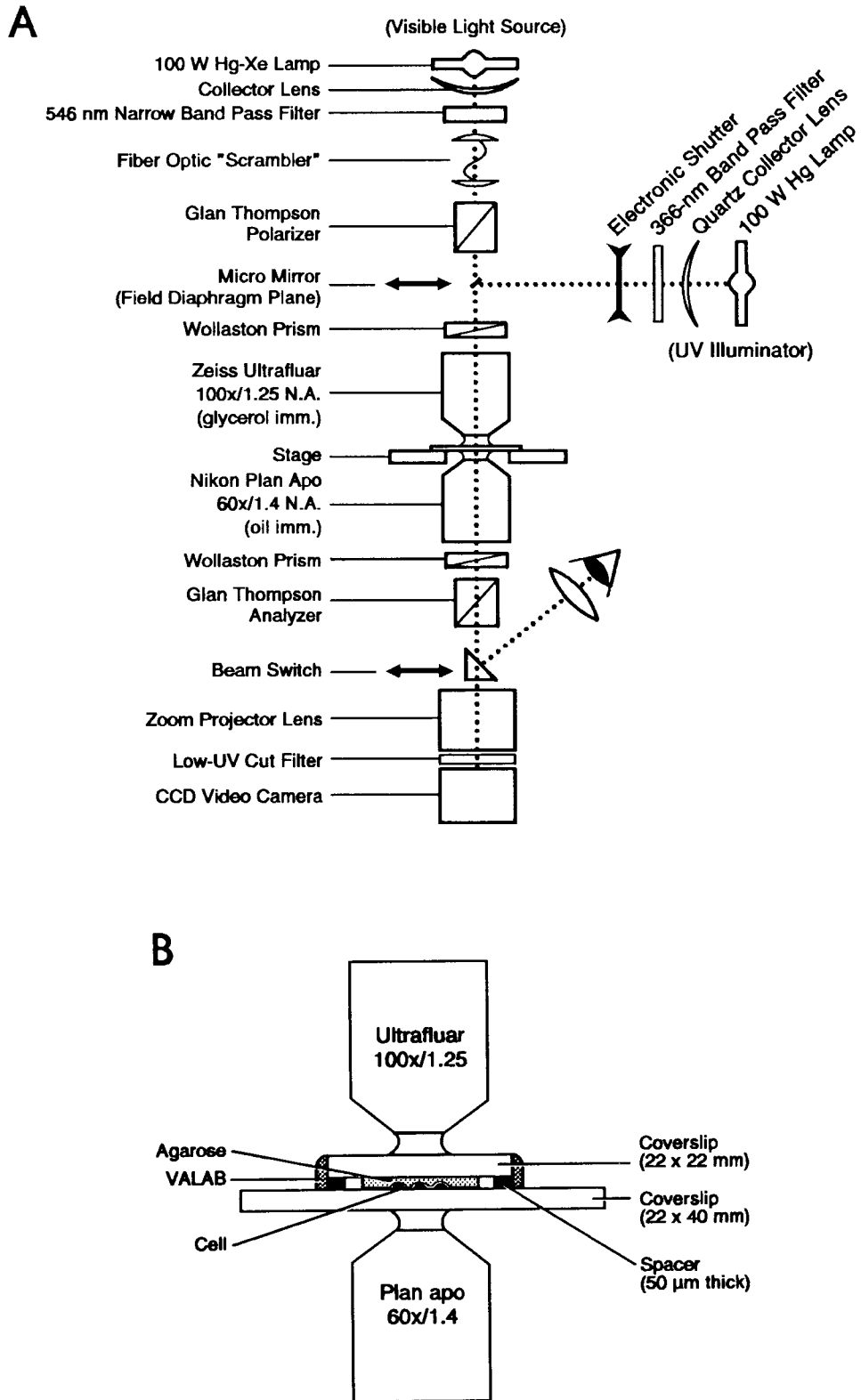


Fig. 1. Diagrams showing the microscope system. **a:** A schematic drawing of the universal polarizing microscope with an attached auxiliary UV illuminator. The UV, reflected from a minute first-surface mirror, is focused by a Zeiss Ultrafluor lens to produce a microspot that releases cAMP from c²AMP. The basic system is similar to that described in Walker et al. [1989]. For detail, see Material and Methods. **b:** Diagram of the observation chamber. Note that the vertical and horizontal scales are not proportional. The amoebae are placed between

a glass coverslip and a small (5 x 5 mm²) piece of 50 μ m-thick agarose sheet which is saturated with 100 μ M c²AMP in 5 mM Hepes buffer (pH 6.7). A Mylar spacer with a circular opening (12 mm in diameter) prevents the sample from being excessively flattened and provides air space around the agar. In addition to providing excellent optical conditions for microscopy, the amoebae sealed in this chamber survive for several days. The lower coverslip is glued on an aluminum holder (not shown) and placed on the stage of the inverted microscope.

Chester, PA), edited using Photoshop (Adobe Systems, Inc., Mountain View, CA) and printed using a dye sublimation printer (model Phaser-II SDX; Tektronix, Wilsonville, OR).

Immunofluorescence Microscopy

For immunofluorescence, the samples were fixed with methanol containing 1% formaldehyde for 5 min at -15°C , and washed with phosphate-buffered saline (PBS: 138 mM NaCl, 2.5 mM KCL, 8 mM Na_2HPO_4 , 1.5 mM KH_2PO_4 , pH 7.2) three times for 5 min each. Primary antibody was applied to the samples and incubated for 30 min at 36°C . The samples were then washed with PBS three times for 5 min each. Secondary antibody was applied to the samples and incubated for 30 min at 36°C . The stained samples were then washed with PBS three times for 5 min each, followed by a brief rinse with distilled water. For double staining with rhodamine-phalloidin (rh-ph), rh-ph was mixed with secondary antibody at a final concentration of $3\ \mu\text{M}$. The samples were mounted with the mounting medium made of a 1:2:4 mixture of polyvinyl alcohol, glycerol and PBS containing 1% (w/v) of an anti-oxidant DABCO (diazabicyclo[2.2.2]octane) (Aldrich Chemical Co., Milwaukee, WI). For fluorescence microscopy, a Zeiss Axioskop-50 or Photomicroscope-III (Carl Zeiss, Inc., Thornwood, NY) equipped with a 63x, NA 1.4 plan apo objective was used. The image was recorded through a cooled CCD camera (model PXL; Photometrics, Tucson, AZ) equipped with Kodak KAF1400 chips, or onto Kodak Tmax-400 monochrome negative films.

Chemicals and Probes

Caged cAMP ($c^2\text{AMP}$; adenosine-3', 5',-cyclic monophosphate, P^1 -[2-nitrophenyl]-ethyl ester) with an absorption maximum at 350 nm was obtained from Calbiochem (La Jolla, CA). A mouse monoclonal anti-*Dictyostelium* myosin [DM-2; Yumura and Fukui, 1985] and a mouse monoclonal anti-*Dictyostelium* actin (HB-80; ATCC) were produced in our laboratory. A rabbit polyclonal anti-*Dictyostelium* myosin-I primarily recognizing myoB was generated by Dr. Thomas Lynch in Dr. Edward Kohn's laboratory at NIH [Fukui et al., 1989]. The mouse monoclonal anti-*Dictyostelium* α -actinin [Schleicher et al., 1988; Witke et al., 1992] and mouse monoclonal anti-*Dictyostelium* talin [Kreitmeier et al., 1995] were generously provided by Dr. Michael Schleicher (Ludwig-Maximilians University, Germany), and Dr. Günther Gerisch (Max-Planck-Institute, Germany), respectively. The rhodamine-labeled phalloidin (rh-ph) was obtained from Molecular Probes, Inc. (Eugene, OR).

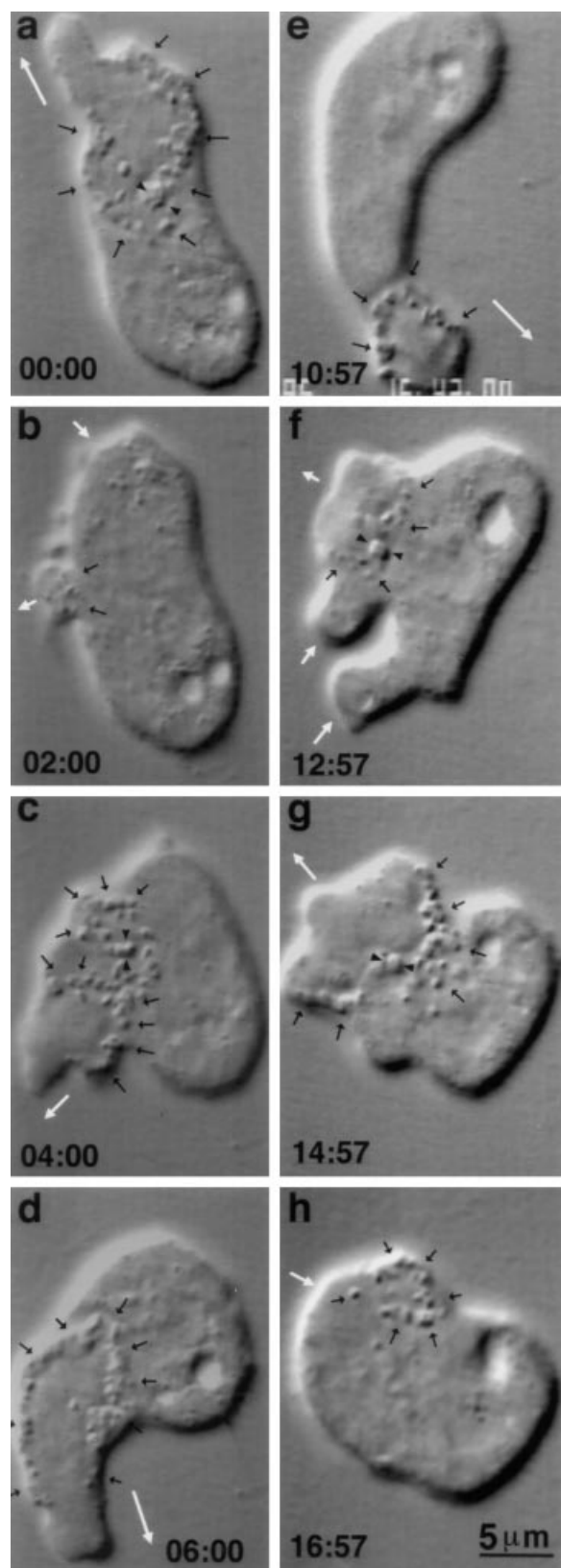
RESULTS

Knobby Feet in the Stationary Stage Amoebae

The amoebae which were prepared between the agarose sheet and coverslip were flattened to different degrees. For example, stationary stage amoebae (between the vegetative and aggregation stages) shown in Figure 2, had an overall thickness of only about $3\ \mu\text{m}$. At mid focus, they clearly displayed several types of organelles (mitochondria and different sizes of vesicles and granules) actively streaming to and from the jaxtanuclear centrosome, located half way between the two nucleoli. The depth of field of the high (condenser and objective) NA DIC system we used was sufficiently shallow (less or equal to $0.3\ \mu\text{m}$) that these organelles became completely blurred or disappeared from view when the focus was "lowered" to the surface of the amoebae contacting the surface of the agarose layer (Fig. 3d). Instead, at that focus, we discovered the presence of small, knobby cortical structures that pressed into the agarose layer Fig. 3e).

The stationary stage amoebae actively protruded and retracted large pseudopodia. Occasionally, the amoebae formed more than one pseudopodium, but only one of them continued to develop while the others retracted prematurely. Full development of the pseudopodium took about 30 seconds. When a flattened amoeba protruded a pseudopodium, it produced knobby cortical structures at the cell-agarose interface (Fig. 2; small black arrows). The initial appearance of a single or two knobs was followed by the formation of multiple knobs (Fig. 3d,e). The size of the knobby feet was $0.95 \pm 0.21\ \mu\text{m}$ ($n = 50$) in cross section. Occasionally they appeared to be larger possibly due to close aposition (Fig. 2a,c,f,g; arrowheads). The knobby feet remained absolutely stationary relative to the substratum and never displayed lateral movement.

Interestingly, the knobby cortical structures usually exhibited an arc-like arrangement at the base of pseudopodium with the opening of the arc pointing towards the direction of the forming pseudopodium (Fig. 2a,c,d,e,g; white arrows, Fig. 3d,e). Within 30 seconds, the pseudopodium reached its maturity and started to retract. Coincidentally, the number and the size of the knobby cortical structures decreased, and they completely disappeared when a new pseudopodium developed from different parts of the cortex (Fig. 2b,f). The flattened shape of the pseudopodium (lamellipodium), the timing of formation and disappearance of the knobby cortical structures, and their stationary location relative to the substratum suggested that they play a role in anchoring the base of the forming lamellipodium to the substratum to help the pseudopodium penetrate into tight spaces. The relative positions of eupodia to pseudopodium is schematically



shown in the diagram viewed from the side of the sample (Fig. 4a).

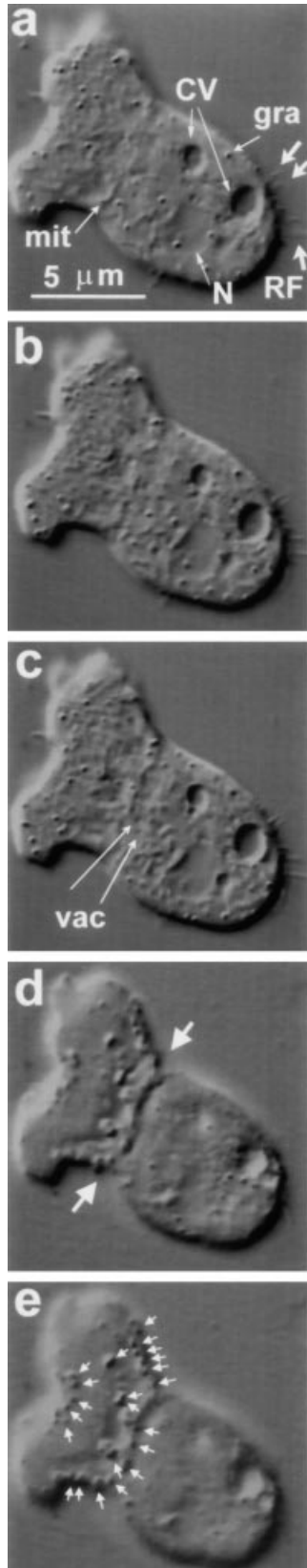
We defined the surface of the amoeba contacting the agarose as ventral because the amoeba always remained attached on this side even when the depth of the medium was as high as 20 μm and almost the entire body was exposed to the fluid. In such cases, the amoebae stayed on the agarose surface and exhibited dynamic three-dimensional (3-D) shape changes by stretching multiple pseudopodia (lobopodia and filopodia) towards the fluid phase between the agarose and glass surfaces. When the pseudopodia contacted the glass surface, the amoebae quickly retracted the pseudopodia. Usually, such amoebae had a “euroid” (a globular, cytoplasmic appendage attached to the rear cortex of the amoeba) and several “retraction fibers” (long, straight, spiny structures attached to the euroid or the rear cortex).

Induced Feet in Aggregating Amoebae

We then used aggregation stage amoebae and induced cAMP-mediated chemotaxis by pulsed UV-microbeam irradiation of caged cAMP (c^2AMP) that was applied to the agar. This new technique allowed us to explore the spatial and temporal relationships between the dynamics of pseudopodial extension and formation of the knobby cortical structures, or feet.

When the microbeam, $1.5 \times 3.5 \mu\text{m}^2$ at the focal plane, was placed about 5–10 μm to the side and front of an aggregation-competent amoeba (Fig. 5a), the amoeba responded by 1) extending a lobopodium towards the pulsed UV spot, 2) completely turning towards, then 3) covering the focused UV microbeam (Fig. 5b), the source of cAMP. This behavioral response was consistent with the cAMP-mediated chemotaxis observed by application of cAMP through a micropipette, particularly the two-step responses originally observed by Swanson and Taylor [1982]. The chemotactic effects of UV flashes were specific to released cAMP since, unlike aggregation stage amoebae, stationary stage amoebae (which do not

Fig. 2. Time lapse sequence showing the dynamics of eupodia formation in a stationary stage amoeba flattened to ca. 3 μm thickness between the coverslip and agarose sheet. Visualized at the amoeba-agarose interface using the very shallow depth of field (ca. 0.3 μm) achieved in our DIC system that provides an exceptionally high objective and condenser NA (= 1.4). **a–d**: Sequence during the first 6 min printed once every 2 min. **e–h**: Sequence of the same amoeba starting at ca. 5 min after panel d. Note that new eupodia, or knobby cortical feet (small black arrows) are formed aligned in an open arc at the base of each newly forming pseudopodium. Each foot is about 1 μm in diameter and does not change its position relative to the substratum. Some feet appear larger perhaps due to close apposition (arrowheads; a, c, f, g). The feet are resorbed as the amoeba retracts the pseudopodium. White arrows indicate the direction of forming or retracting pseudopodia. Time in min:seconds. Scale bar = 5 μm .



have cAMP receptors and therefore are insensitive to cAMP) did not show any response. Furthermore, amoebae in neither stage responded to UV microbeam flashes applied in the absence of c²AMP.

In the monopodial, aggregation stage amoebae that were relatively unflattened and which continued to migrate (cell #1 and #2), we did not observe the formation of knobby feet (Fig. 5a,b). Our observation on the stationary stage amoebae (Fig. 2), nevertheless, suggested that knobby feet are essential when firm anchorage of the cell to the substratum is required.

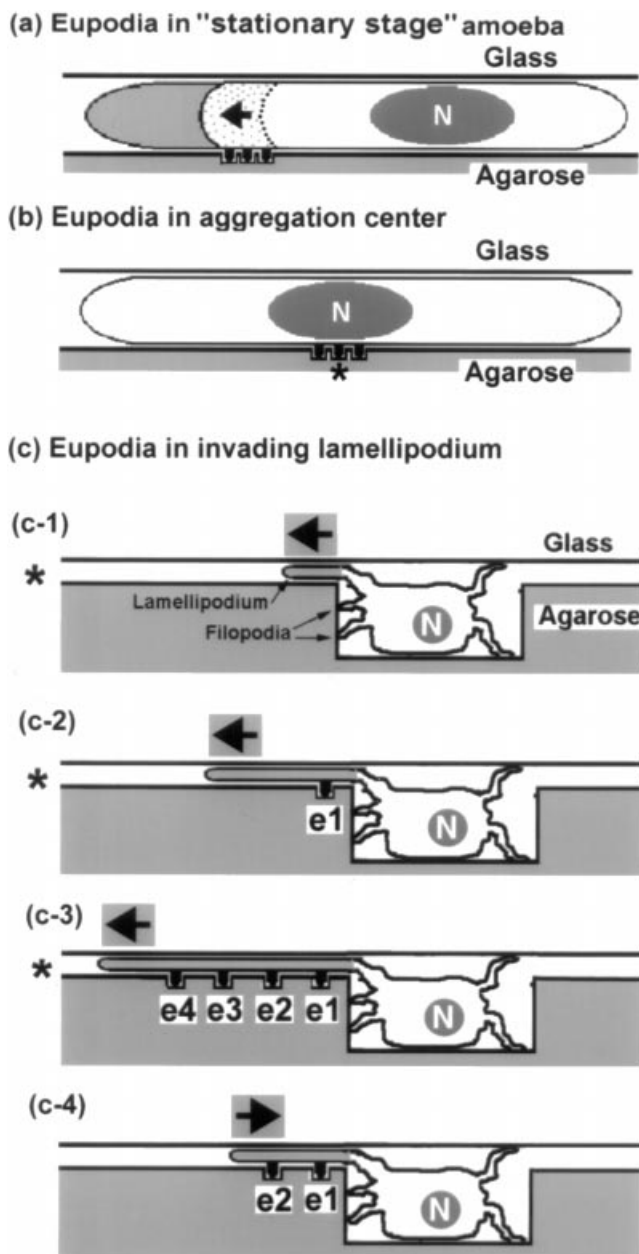
The above suggestion was reinforced by observing the amoeba that was located at the center of an induced aggregation, immediately beneath the UV-microbeam (Fig. 5c,d). When the microbeam was precisely focused at the amoeba-agarose interface, the centrally-located amoeba stopped migrating, became frozen in location and extended into a disk shape (cell #1 in Fig. 5c). At this point, the amoeba, which has become flatter than the migrating monopodial amoebae, form knobby feet at the lower middle surface just beneath the microbeam (arrows in cell #1 in Fig. 5d; diagram in Fig. 4b). When the microbeam was turned off, the feet disappeared within a matter of a minute and the amoeba became motile again (Fig. 5d,e). The induction of the feet was reversible; when the UV flashes were restarted, they reappeared very rapidly under the beam center. Irradiation of the UV microbeam with 30 msec exposure and 650 msec interval for at least a half hour did not cause any visible damage to the amoebae.

As shown in Figure 5, amoebae other than the central one just described, also responded to cAMP and formed an “aggregate” by surrounding the first amoeba now affixed beneath the microbeam. Continuous, long term observations showed that the surrounding amoebae, which remained more elongated and did not form knobby feet, exhibited a swirling movement around the central amoeba. As long as the UV flashes continued, the aggregate continued to increase in size until several scores of amoebae swirled in a stream around the central affixed amoeba.

Fig. 3. A through-focus series of DIC images showing that the knobby feet project into the agarose matrix. The panels represent frozen frames selected from a video rate recording of optical sections of a total of 3.5 μm z-axis movement of the microscope stage. The height of the section from the dorsal surface is 0.5 μm (a), 1.5 μm (b), 2.5 μm (c), 3.0 μm (d), and 3.3 μm (e). In the middle cytoplasm (b,c), numerous organelles show saltatory (gra, vac) or random (CV, N) modes of movement. At the ventral cortex contacting the surface of agarose (d), an array of the knobby feet (“eupodia”) exhibits a continental fold-like appearance (large arrows). Focusing 0.3 μm below from the ventral surface (e), the unitary appearance of eupodia (small arrows) becomes obvious. Also note a mottled appearance of the agarose matrix surrounding the eupodia (e). CV: contractile vacuole; gra: granule; mit: mitochondrion; N: nucleus; RF: retraction fiber; vac: vacuole. Scale bar = 5 μm.

Dynamics of the Knobby Feet Formed in Thin Lamellipodia

A key evidence for the role played by the knobby feet in amoeba-substratum anchorage was achieved by observing amoebae that projected extremely thin lamellipodia into a tight space (Fig. 6; schematic side view in Fig. 4c). Amoebae crawling in a naturally formed channel in the agarose were induced to project lamellipodia into a thin space between the coverslip and agarose adjacent to the channel. When the microbeam source of cAMP was placed at about 5–10 μm from the channel, the amoeba responded by 1) ceasing its migration (Fig. 6a), 2) forming several filopodia and lamellipodia at time 0:10,

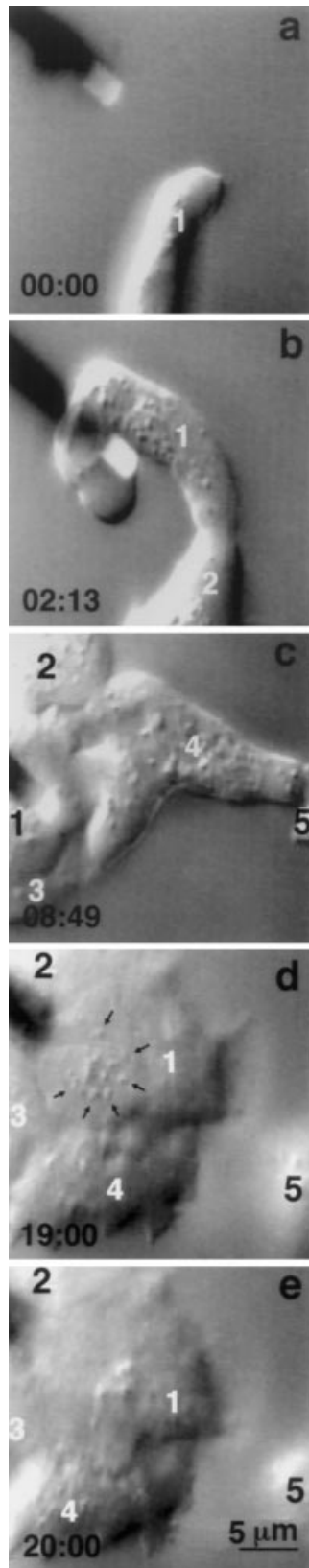


and 3) extending an extremely thin lamellipodium towards the image of the UV beam (Fig. 6b; schematic side view in Fig. 4c-1). Coincidentally, knobby feet were formed on the penetrating lamellipodium (arrows in Fig. 6b,c; schematic side view in Fig. 4c-2 to c-3). The knobby feet quickly disappeared when the UV microbeam was turned off and as the lamellipodium started to retract (Fig. 6d,e; schematic side view in Fig. 4c-4). Again, the position of the feet was fixed relative to the substratum and showed no sign of lateral movement. When the c²AMP uncaging UV microbeam was activated again, the retracting lamellipodium re-expanded towards the cAMP source as it formed new knobby feet. Thus, there is a close correlation between feet formation and invasive extension of the lamellipodium.

Cytoskeletal Organization of the Feet

In bright field microscopy of fixed amoebae, the knobby feet, or eupodia, appears as dark bodies indicating their high refractive index (Fig. 7a,d,g). Immunofluorescence staining demonstrates that the feet are highly enriched in the major cytoskeletal component actin (Fig. 7b). Staining with rh-ph showed that most actin in the feet is filamentous (F-actin) (Fig. 7e,h). Double-staining for actin and myosin-I demonstrated that myosin-I (myoB) is also localized in the feet. Myosin-I exhibits a ring-like structure, indicating that it is concentrated at the periphery of the feet (Fig. 7b,c). In contrast, α -actinin shows a pattern of homogeneous staining within the feet suggesting a more uniform association with F-actin filaments located there (Fig. 7e,f). Certain variations in the occurrence between F-actin and myosin-I as well as F-actin and α -actinin were noted. Particularly interesting was that some of the knobby feet only showed high accumulation of F-actin, but not of myosin-I (arrowhead, Fig. 7a-c).

Fig. 4. Schematic diagrams of flattened amoebae with eupodia in side view. **a:** Naturally forming eupodia at the base of an extending pseudopodium in randomly moving "stationary stage" amoeba. The schematic corresponds to the image shown in Figure 2e. **b:** Eupodia induced beneath the source of cAMP at the ventral surface of the aggregation stage amoeba located in the center of the swirling aggregate. The schematic corresponds to Figure 4d. **c:** Eupodia formed on a very thin lamellipodium invading into a narrow space. The amoeba stops in the channel and extends its lamellipodium towards the source of cAMP released by the UV-microbeam. **c-1:** The lamellipodium begins to invade into the thin space. **c-2:** The first eupodium is formed. **c-3:** As the lamellipodium continues to develop, more eupodia are formed. Some of them disappear while others are formed; but they do not show any lateral movement relative to the substratum. **c-4:** The lamellipodium is retracting as the UV flashes have been turned off and the amoeba retreats to the channel. The eupodia disappear as the lamellipodium retracts. The image sequence is shown in Figure 5. The figures in (c) are drawn smaller than those in (a) and (b). For simplicity, the drawing of the cell body in c-1–c-4 does not show its dynamic shape changes. Arrows a,c = direction of expansion of lamellipodium. N: nucleus. *: c²AMP uncaging UV flashes. (e-1–e-4): eupodia.

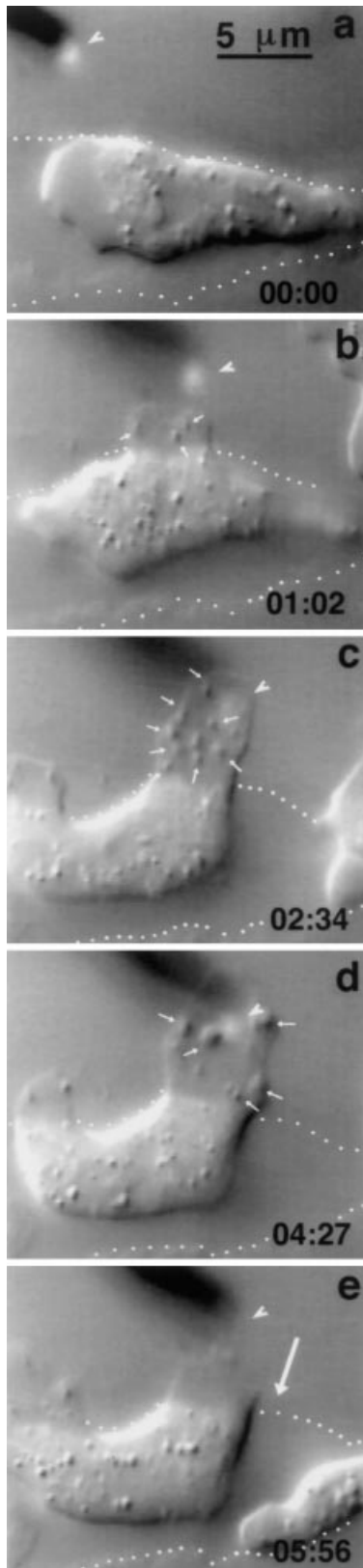


The localization of a talin homologue of *Dictyostelium* was determined by using two mouse monoclonal antibodies: 1) mab 169-477-5 raised against purified *Dictyostelium* talin [Kreitmeier et al., 1995], and 2) mab 227-341-3 raised against a fusion protein containing N-terminus of *Dictyostelium* talin [Jens Niewöhner, Max-Planck-Institute, unpublished]. Both antibodies showed primarily diffuse cytoplasmic staining with a higher accumulation at the cortex (Fig. 7i). Double staining with rh-ph demonstrates that *Dictyostelium* talin is not concentrated at the eupodia (Fig. 7h,i).

These results reveal that the knobby feet are rich in F-actin associated with actin-binding proteins such as myosin-I and α -actinin. In contrast, a *Dictyostelium* homologue of talin is not concentrated in the eupodia. We have also examined the localization of conventional myosin (myosin-II) and find that it is not concentrated in the eupodia (data not shown).

At high resolution, fluorescence micrographs demonstrate that F-actin is disposed in a radial array after emerging from the eupodia (Fig. 8). It appears that most of these radially arrayed F-actin filaments run parallel to the ventral cortex. Some of the filaments appear to interact with others from neighboring eupodia at the periphery of the radial array (curved arrow in a; double arrows in b). Actin filaments also interact with the axial bundle of F-actin cables emerging from the tip of the lamellipodium (arrowheads, a,b) suggesting the presence

Fig. 5. Chemotaxis towards uncaged cAMP, and eupodia formation in an amoeba located at the center of a forming aggregate. When activated, the electronic shutter was opened for 30 msec every 650 msec exposing the preparation to intermittent 366-nm UV microbeam, approximately $1.5 \times 3.5 \mu\text{m}$ in size. The microbeam released cAMP from the agarose containing $100 \mu\text{M}$ cAMP and acted as the source of a transient gradient of cAMP which should dissipate rapidly. The microbeam (white rectangle) was located somewhat above the center of the field in panels a and b. The dark rod is the shadow of the metal arm supporting the micromirror whose actual size was about $150 \times 350 \mu\text{m}$ (see Fig. 1). **a:** The image of the micromirror was placed about $10 \mu\text{m}$ to the side of the anterior lobopodium of cell #1 and pulsed irradiation started. **b:** The amoeba turned to the beam where the uncaged cAMP was released and started a spiral motion around the beam center. A second cell (#2) followed the first cell (#1). **c:** The same amoeba (#1) stopped migrating, changed shape from elongated to pancake shaped, and stayed just beneath the UV beam. Note that other amoebae (#2-5) were also attracted to the cAMP source (or cAMP released from congregating amoebae) and started to form a small aggregate encircling the first amoeba. **d:** In cell #1, a group of eupodia was formed beneath the UV microbeam (which had been turned off and removed from the field just 3 sec before this frame was recorded). Small black arrows point to representative eupodia. **e:** 63 sec after the UV microbeam was turned off. The eupodia are disappearing. In (a-c) focused near the mid-plane of the amoeba, organelles are visible. No eupodia are present at this stage. d,e: Focused at the agar-amoeba interface, show the eupodia that are present only in cell #1 during, and for a short while after, cAMP is released by the UV microbeam. Time in min:sec. Scale bar = $5 \mu\text{m}$.



of mechanical linkage between eupodia and the lamellipodium through F-actin cables. Interestingly, several long, very thin, F-actin-containing fibers were also observed, connecting the eupodium and the leading edge of the pseudopodium, as represented by the one indicated by the triple small arrowheads in Figure 8b.

DISCUSSION

Is Eupodium a True Foot?

As demonstrated in this study, the knobby feet are stationary relative to the substratum and never show lateral movement. This structure usually appears as multiple units arranged approximately in an arc of a circle opened in the direction of a forming lamellipodium invading a narrow space. They disappear as the lamellipodium retracts. The knobby feet also formed at the ventral surface of an aggregation stage amoeba, located and anchored in the center of an aggregate just above the cAMP uncaging UV microbeam. Other amoebae lacking knobby feet continued to actively swirl around this central amoeba. The knobby feet were resorbed and the central amoeba began to migrate again very soon after the UV microbeam was turned off.

Thus the knobby feet are formed only when a firm cell-substratum anchorage appears to be required. These characteristics suggest an obvious function of eupodia, i.e., transient anchorage to deformable substratum. Therefore, we named this structure eupodium. In natural habitat, we believe the eupodia could anchor pseudopodia that extend into tight spaces when the amoebae crawls in the soil and amidst rotten leaves. The absence of eupodia in rapidly moving aggregation stage amoebae suggest that amoebae in that stage use locomotory mechanisms

Fig. 6. Dynamics of eupodia formed on a thin lamellipodium invading an exceptionally narrow space between agarose and coverslip. **a:** An aggregation stage amoeba exhibiting a monopodial lobopodium and migrating to the left of the field along a narrow channel in the agarose. A $1.5 \times 2.5 \mu\text{m}^2$ UV microbeam (white arrowhead) was placed to the side of the channel and 3 msec pulses started 18 sec before this frame. **b:** A thin lamellipodium projects toward the source of the uncaged cAMP. The small white arrows point to the first three eupodia developing. **c:** The lamellipodium has reached the microbeam as prominent eupodia are formed (white arrows). **d:** The thin lamellipodium exhibited dynamic shape change during the 2 min period between c and d, and eupodia were formed at different positions (small arrows). **e:** The UV microbeam was turned off within 1 second after (d). The lamellipodium is quickly retracting and coincidentally all the eupodia are disappearing. All of the spherical structures other than eupodia are organelles in the endoplasm as determined by through focus observation. In contrast to the eupodia whose locations do not change, the organelles actively move around in the endoplasm; only those that are within $0.3 \mu\text{m}$ of the focal plane are imaged. Arrowhead: UV microbeam releasing cAMP. Dotted line: edge of the channel. Small arrows: eupodia. Large arrow: retracting lamellipodium. Time in min:sec. Scale bar = $5 \mu\text{m}$.

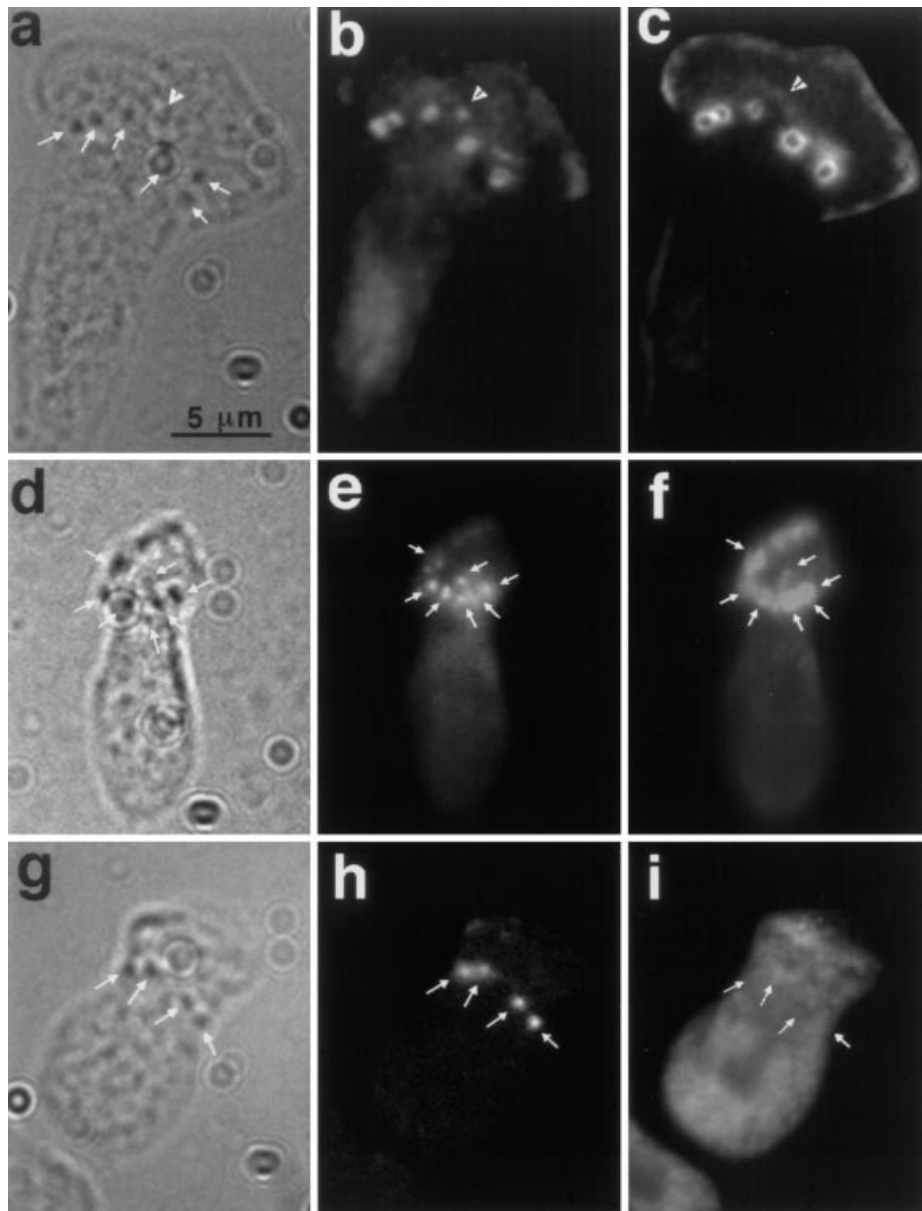


Fig. 7. Immunofluorescence localization of actin and related cytoskeletal components at the eupodia of the stationary stage amoebae. a–c: Double staining for actin and myosin-I. **a**: Bright field. **b**: Actin as stained with a mouse monoclonal anti-*Dictyostelium* actin. **c**: Myosin-I (myoB) as stained with a polyclonal anti-*Dictyostelium* myosin-I. Myosin-I shows a ring-like distribution indicating that it is located beneath the membrane of the eupodium. One eupodium (arrowhead) is rich in F-actin (**b**), but not in myosin-I (**c**), indicating that these cytoskeletal components may be integrated into, or leaving, the

eupodium at different times. d–f: Double staining for F-actin and α -actinin. **d**: Bright field. **e**: F-actin as stained with rh-ph. **f**: Staining with a mouse monoclonal anti-*Dictyostelium* α -actinin demonstrating that it is highly concentrated throughout the eupodium. g–i: Double staining for F-actin and talin. **g**: Bright field. **h**: F-actin as stained with rh-ph. **i**: Staining with a mouse monoclonal anti-*Dictyostelium* talin showing that *Dictyostelium* talin is not concentrated at the eupodia. Arrows: eupodia. Scale bar = 5 μ m.

similar to leukocytes moving in a non-invasive mode, i.e., by simple pseudopodial projection and retraction [Kolega et al., 1982].

Is Eupodium a *Dictyostelium* Adhesion Plaque?

The eupodium is a structure distinctive from adhesion plaques of higher organisms based on the following

criteria. 1) While adhesion plaques are always attached to stress fibers, *Dictyostelium* does not form stress fibers. 2) While it takes at least 180 min for adhesion plaques to establish, eupodia is formed in less than 2 min. 3) While adhesion plaques are only formed on solid substratum (but not in collagen gel) [Burridge et al., 1988], eupodia are formed on partially deformable substratum. 4) While

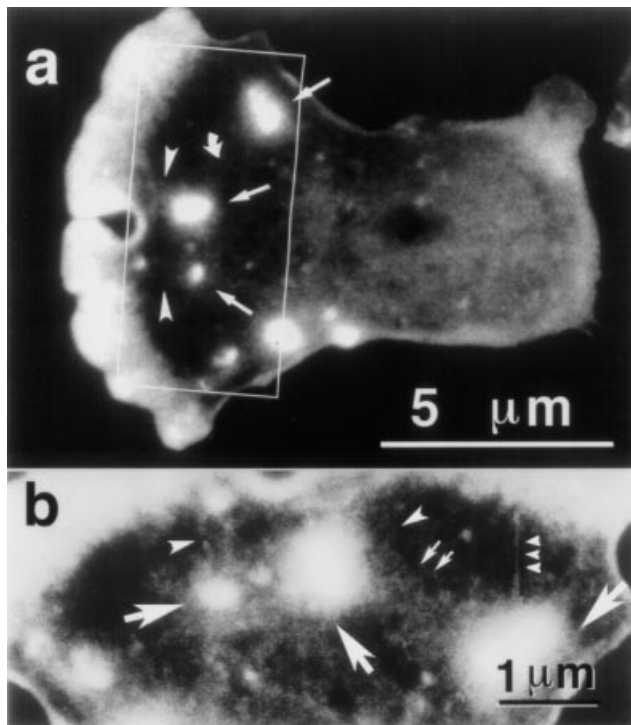


Fig. 8. High-resolution fluorescence micrographs showing actin filaments' organization as demonstrated by staining with rh-ph. **a:** Whole amoeba showing F-actin distribution in this flat, monopodial amoeba moving to the left. There is a prominent staining of F-actin: within and around eupodia (long arrows); in the anterior lamellipodium (left); and in the cortex, with a high accumulation at the tail end (right). The staining indicates that F-actin (arrowheads) from the eupodia interacts with F-actin from lamellipodium and also (curved arrow) from another eupodium. **b:** Lighter print at higher magnification of the rectangular area marked in (a). Double small arrows show the F-actin arrays emanating from eupodia that are interacting with other arrays. Arrowheads show bundles of F-actin filaments connecting a eupodium and the lamellipodium. Note that there are also long, very thin F-actin filaments connecting a eupodium such as one represented by the triple small arrowheads. Arrows: Eupodia.

adhesion plaques are rich in talin, eupodia are not. The eupodia contain myosin-I instead.

Superficially, eupodia share certain common properties with a specialized form of adhesion plaques, or "podosomes." First, podosomes are formed by specific cells that are invasive in nature, including RSV-transformed fibroblasts [Tarone et al., 1985; Nermut et al., 1991], bone resorpting osteoclasts [Lakkakorpi and Väänänen, 1991], and neutrophils penetrating into endothelial layer of blood vessels [Wolosewick, 1984]. Recent studies revealed that certain podosomes formed by cancer cells ("invadopodia") secrete proteases to dissolve fibronectin matrix of the basement membranes [Mueller et al., 1992]. Second, podosomes are more dynamic than adhesion plaques as revealed by 1) fluorescence recovery after photobleaching and 2) fluorescent analogue cytochemis-

try of actin, vinculin and α -actinin [Geiger et al., 1984; Stickel and Wang, 1987]. Furthermore, like eupodia, podosomes are protrusions rather than contact sites [David-Pfeuty and Singer, 1980; Mueller et al., 1992]. However, the *Dictyostelium* eupodia we discovered are distinct from podosomes in that eupodia provide anchorage for invasive extension of pseudopodium. In contrast, podosomes of themselves are reported to transform into invasive projections rather than providing anchorage to other projectile cortical structures [Wolosewick, 1984]. Whether eupodia are also formed by other amoeboid cells is yet to be determined.

Cytoskeletal Organization of the Eupodium

The present study shows that eupodia are most often formed at the base of newly forming pseudopodia (Fig. 2). Fluorescence microscopy also demonstrates that the eupodium contains a large amount of F-actin (Figs. 7 and 8). It appears that F-actin from the eupodium emerges as a radial array and interacts with the "axial" bundle of F-actin arising from the leading edge of the lamellipodium (Fig. 8). It is intriguing to speculate that this interaction may somehow provide a mechanical base to overcome physical resistance produced at the forming, leading edge, of the pseudopodium (see next section). The F-actin cables in a radial array originating from a eupodium also appear to interact with those from other eupodia if they are located within a distance of 3–5 μ m (Fig. 8).

This study also demonstrates that the cortex of the eupodium contains a high concentration of myosin-I. *Dictyostelium* myosin-I, more specifically myoB and myoD, has been localized at the leading edges of migrating amoeba or in the polar lamellipodia of dividing amoeba [Fukui et al., 1989; Jung et al., 1993]. It has also been localized in the apex of filopodia [Morita et al., 1996]. Structurally, this class of myosin has two actin-binding sites, one of which (in the head domain) is ATP-sensitive, and the other (in the tail domain), insensitive. It also has a putative membrane-binding domain in the rod [Hammer, 1991; Titus et al., 1994]. Thus, although yet to be demonstrated, one possible activity of myosin-I is to crosslink F-actin to the plasma membrane so that ATP hydrolysis induces mutual sliding between F-actin and the plasma membrane.

Myosin-I from *Acanthamoeba* also crosslinks F-actin and forms a gel. The gel contracts when ATP is added [Fujisaki et al., 1985]. However, unlike myosin-II, myosin-I does not form bipolar arrays that can induce sliding between oppositely polarized actin filaments [Korn, 1982; Pollard et al., 1991].

Our immunofluorescence localization demonstrates that myosin-I exhibits a ring-like pattern in the eupodia (Fig. 7a–c). This evidence suggests that myosin-I may

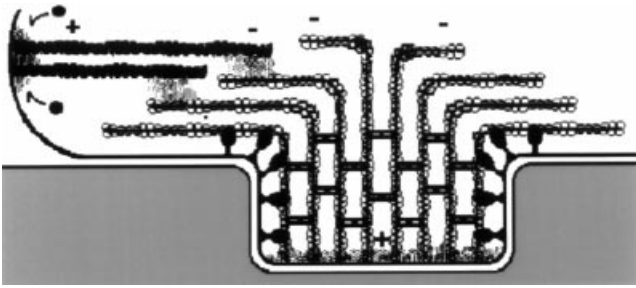


Fig. 9. Schematic diagram illustrating the side view of an eupodium. Only some representative actin filaments are illustrated. This model reflects the findings from fluorescent antibody localization and the fact that the eupodium is a highly condensed structure formed at the cortex of the cell contacting a deformable surface. The eupodium contains a concentrated bundle of F-actin crosslinked by α -actinin homodimers (lateral rods). After emerging from the eupodium, the actin filaments turn parallel to the ventral surface and form a radial array. Myosin-I (black oval with rod) interacts with the peripheral actin filaments and the plasma membrane surrounding the eupodium. Actin filaments are illustrated in black or white indicating that they originate from different membrane domains. The nature of the materials linking the two groups of actin filaments to each other, and their plus ends (?) to the plasma membrane, are still unknown. See text for further discussion.

crosslink F-actin to the plasma membrane in a way similar to microvilli of intestinal brush border [Matsudaira and Burgess, 1979; Mooseker et al., 1989]. Although eupodia and microvilli perform different biological functions (anchorage to substratum versus absorption through a contact-free surface), could the similarity in their cytoskeletal organization suggest that the interaction of the myosin heads with an actin bundle support an extensive force for both microvillar and eupodial membrane to which the myosin tails are anchored (see Fig. 9 and next section)? In contrast, eupodia and podosomes appear to be similar in function but differ in their cytoskeletal makeup. To our knowledge, it is not known whether podosomes (and invadopodia) contain myosin-I. It will be interesting to examine this possibility.

We showed that α -actinin is also included in the eupodium. *Dictyostelium* α -actinin was first isolated as a 95 kD gelation factor from an actin enriched fraction [Condeelis and Taylor, 1977]. It has been demonstrated that α -actinin is a calcium-dependent actin-crosslinking protein capable of forming a rod-shaped homodimer of 30–40 nm in length [Fechheimer et al., 1982; Schleicher and Noegel, 1992]. Our immunofluorescence study reveals that there is a high concentration of α -actinin in the eupodium (Fig. 7d–f). It is very likely that α -actinin in the eupodium bundles F-actin as illustrated by the model shown in Figure 9. We are tempted to predict that there will be defects in eupodia formation and invasive extension of pseudopodia in α -actinin mutants, even though a gene targeting disruption of this protein showed little defect affecting general cell motility [Witke et al., 1992].

How Do Eupodia Function?

We have shown that the *Dictyostelium* amoeba produces eupodia when it appears necessary to anchor a cell in the middle of a swirling aggregate, or otherwise to secure the amoeba to the substratum when invading a narrow space. Thus we postulate that the eupodia are transiently formed anchoring feet that secure the amoeba to the substratum, and which counteracts the reactive force encountered by a lamellipodium that is experiencing resistance to its protrusion.

We have also shown, as schematically illustrated in Figure 9, that the core of the eupodium contains a highly concentrated bundle of F-actin that appears to be crosslinked by α -actinin homodimers. Myosin-I is found in the eupodial cortex where it may well crosslink the core F-actin with the plasma membrane of eupodium. After emerging from the eupodium, the actin filaments splay out into a radial array with their minus, slow growing ends pointing radially. The splayed eupodial actin filaments are disposed as though interacting with actin filaments arising from the leading edge of the lamellipodium.

Coupled with the arrangements of these molecular components, the total lack of any motion within the eupodium (even under the highest resolution of the light microscope), its high refractive index, and timing and location of its formation, leave little doubt that the eupodium is a transiently formed, local, protruding gelled knob formed by concentration of proteins in the cell. It seems perfectly reasonable that such a structure could provide anchoring function. The composition and physical properties of the eupodia tempt us to also suggest that they may be induced by highly localized influx and/or release of Ca^{2+} ions.

While it appears very likely that the eupodium buttresses the protrusive work of a lamellipodium encountering resistance, the exact interactions between the components of the eupodium, cell membrane, and lamellipodium that lead to such buttressing action still needs to be clarified. Nevertheless, the cortical localization of myosin-I surrounding the concentrated core of F-actin and α -actinin in the eupodium, and the apparent interaction of the F-actin cables arising from the eupodium with those in the axial bundle of the lamellipodium, suggest that these interactions may play significant roles in the anchored, stationary eupodia countering the reactive force needed for the lamellipodium to invade a narrow space. In this connection, polymerization of the axial bundle of F-actin at its barbed end (i.e., at the leading edge of the pseudopodium) may well be participating in the production of protrusive force. Indeed, such force generation due to actin polymerization has been considered strong enough to bring about protrusive motility in several types of cell extensions [Tilney and Inoué, 1985;

Oster, 1988; Albrecht-Buehler, 1990; Cooper, 1991; Fukui, 1993].

Full elucidation of eupodial components, their molecular organization, and interactions with the cytoskeletal components of the extending pseudopodium, as well as possible interaction of the eupodial elements with its membrane and extracellular matrix, must await further studies.

UV Microbeam Release of cAMP Provides a New Tool for Studying Chemotaxis

Chemotaxis towards cAMP by *Dictyostelium* [Bonner, 1947; Konijn et al., 1969; review, Bonner, 1971] involves a signal transduction pathway including cAMP receptors, adenylate cyclase, cAMP phosphodiesterase, G-proteins, and free calcium to list a few [review, Gerisch, 1982, 1987; Devreotes, 1989].

It has been shown by cinemicrographic analysis of migrating amoebae, that there is a relay mechanism between amoebae involving the successive release of cAMP, which is propagated radially with a "unitary zone" of 57 μm and a relay time of 12 seconds [Alcantara and Monk, 1974]. The response of amoeba to a single pulse of cAMP is as fast as 5 seconds and the amoebae move about two-cell lengths over a period of 50–100 seconds [Gerisch, 1979]. Binding of cAMP with the receptors triggers synthesis followed by an emission of cAMP to the extracellular space occurring within 12 seconds after the binding [Alcantara and Monk, 1974; Roos et al., 1975]. It is also known that emitted cAMP is destroyed by extracellular phosphodiesterase before it travels for 60 μm so that each time an amoeba emits cAMP, it produces a gradient [Roos et al., 1975; Gerisch, 1976]. In his pioneering work, Gerisch suggested need for cAMP oscillation for the sensing mechanism in chemotaxis [Gerisch, 1979].

In buffer solution containing a high density ($2 \times 10^8/\text{ml}$) of aggregation competent amoebae, naturally occurring oscillation of cAMP with highest concentration of $1\text{--}2 \times 10^{-6}$ M and peak duration of 3–10 min have been determined [Gerisch and Wick, 1975]. An amoeba has $10^5\text{--}10^6$ cAMP receptors with a half-maximum kd of 2×10^{-7} M [Gerisch et al., 1975; Gerisch and Malchow, 1976; review, Gerisch, 1987; Klein et al., 1988]. In suspension, a stimulation with 2×10^{-9} M cAMP results in a ten-fold amplification of the extracellular cAMP [Roos et al., 1975]. There is also a Ca^{2+} influx stimulated by cAMP uptake by amoebae [Wick et al., 1978].

The spiral aggregation pattern observed in this study seems to reflect a pattern of cAMP propagation caused by the combination of pulsed uncaging of cAMP and the cAMP secreted by amoebae. Initially, uncaged cAMP should propagate in a radial pattern by diffusion, and this gradient attracts the first amoeba. The amoeba,

unless pointing directly towards the gradient source, should spiral in towards the source following a repeatedly appearing uphill gradient in a mathematically predictable track. While responding to the cAMP source, the first amoeba emits cAMP from its posterior tail, which generates a new a local wave of cAMP. This local cAMP wave should trigger chemotaxis of a neighboring amoeba towards the first amoeba, and thus the chain elongates when more amoebae are stimulated. When the first amoeba comes to lie immediately over the source of uncaged cAMP, it ceases to move and becomes anchored as it expands into a pancake shape. The other amoebae continue to move around the first amoeba and generate a slow moving spiral pattern. At times, we have observed this spiral containing hundreds of amoebae streaming in the same direction. Such spiral pattern of aggregation would appear to mimic a naturally occurring spiral wave of chemotactic stream observed by Gerisch et al. [1979].

In spite of the accumulated evidence for cytoskeletal reorganization during cAMP mediated chemotaxis, the precise mechanism of the cellular response leading to directional migration has not been elucidated [Futrelle et al., 1982; Yumura and Fukui, 1985; McRobbie and Newell, 1984; Soll, 1988]. For example, the distribution of cAMP receptors has not been determined, and the behavioral responses of the mutants, to date, have not unveiled any critical mechanism.

In our current study, we showed that 3 or 30 msec flashes of 366-nm UV microbeam attracts aggregation-competent *Dictyostelium* amoebae. The effect on the amoebae of the UV microbeam uncaging of cAMP was reversible and could be repeated many times. There was no damage observed up to an hour of continuously pulsed or intermittent irradiation. This demonstrates that the UV microbeam regime that we devised should be useful, not only in generating cAMP gradients effective in attracting the amoebae, but for analyzing the precise distribution of receptors on the individual migrating amoeba. Judging from the response of the amoeba, the concentration of released cAMP must be at least $1\text{--}2 \times 10^{-6}$ M, with a gradient high enough to attract the amoebae [Gerisch and Wick, 1975]. Measurement of the exact concentration, distribution, and the time course of change of the cAMP released by pulsed microbeam irradiation of c²AMP should prove to be very interesting.

CONCLUSIONS

We suggest that the eupodium we discovered in *Dictyostelium* amoebae is a unique anchoring structure distinct from adhesion plaques of higher organisms but may function somewhat similar to podosomes (or invadopodia). The induction of chemotaxis by pulsed UV-microbeam release of cAMP from c²AMP and the obser-

vation chamber we describe should provide powerful new tools for studying the behavioral response, organellar motility and signal transduction mechanisms in these amoebae and other cells. Understanding how a cell recognizes when it needs to form such anchoring structures should reveal interesting biological mechano-sensory mechanisms.

ACKNOWLEDGMENTS

Supported by NIH grants RO1-GM39548 to Y.F. and R37-GM31617 to S.I.

REFERENCES

- Abercrombie, M., J.E.M. Heaysman, and Pegrum, S.M. (1971): The locomotion of fibroblasts in culture. IV. Electron microscopy of the leading lamella. *Exp. Cell Res.* 67:359–367.
- Albrecht-Buehler, G. (1990): In defense of “nonmolecular” cell biology. *Int. Rev. Cyt.* 120:191–241.
- Alcantara, F., and Monk, M. (1974): Signal propagation during aggregation in the slime mould *Dictyostelium discoideum*. *J. Gen. Microbiol.* 85:321–334.
- Bonner, J.T. (1947): Evidence for the formation of cell aggregates by chemotaxis in the development of the slime mold *Dictyostelium discoideum*. *J. Exp. Zool.* 106:1–26.
- Bonner, J.T. (1971): Aggregation and differentiation in the cellular slime molds. *Ann. Rev. Microbiol.* 25:75–92.
- Burridge, K., Fath, K., Kelly, T., Nuckolls, G., and Turner, C. (1988): Focal adhesions: Transmembrane junctions between the extracellular matrix and the cytoskeleton. *Ann. Rev. Cell Biol.* 4:487–525.
- Cocucci, S., and Sussman, M. (1970): RNA in cytoplasmic and nuclear fractions of cellular slime mold amoebas. *J. Cell Biol.* 45:399–407.
- Condeelis, J., and Taylor, D.L. (1977): The contractile basis of amoeboid movement. V. The control of gelation, solation, and contraction in extracts from *Dictyostelium discoideum*. *J. Cell Biol.* 74:901–927.
- Cooper, J.A. (1991): The role of actin polymerization in cell motility. *Ann. Rev. Physiol.* 53:585–605.
- David-Pfeuty, T., and Singer, S.J. (1980): Altered distributions of the cytoskeletal proteins vinculin and α -actinin in cultured fibroblasts transformed by Rous sarcoma virus. *Proc. Natl. Acad. Sci. USA* 77:6687–6691.
- Dejardin, P. (1835): Sur les organismes inferieurs. *Ann. Sci. Nat. Zool.* 4:343–377.
- Dellinger, O.P. (1906): Locomotion of amoebae and allied forms. *J. Exp. Zool.* 3:337–358.
- Devreotes, P.N. (1989): *Dictyostelium discoideum*: A model system for cell-cell interactions in development. *Science* 245:1054–1058.
- Fechheimer, M., Brier, J., Rockwell, M., Luna, E.J., and Taylor, D.L. (1982): A calcium- and pH-regulated actin binding protein from *D. discoideum*. *Cell Motil.* 2:287–308.
- Fujisaki, H., Albanesi, J.P., and Korn, E.D. (1985): Experimental evidence for the contractile activities of *Acanthamoeba* myosins IA and IB. *J. Biol. Chem.* 260:1183–1189.
- Fukui, Y. (1993): Toward a new concept of cell motility: Cytoskeletal dynamics in amoeboid movement and cell division. *Int. Rev. Cyt.* 144:85–127.
- Fukui, Y., and Inoué, S. (1995): Chemotaxis, aggregation behavior, and foot formation in *Dictyostelium discoideum* controlled by microbeam uncaging of cyclic-AMP. *Biol. Bull.* 189:198–199.
- Fukui, Y., and Yumura, S. (1986): Actomyosin dynamics in chemotactic amoeboid movement of *Dictyostelium*. *Cell Motil. Cytoskel.* 6:662–673.
- Fukui, Y., Lynch, T.J., Brzeska, H., and Korn, E.D. (1989): Myosin I is located at the leading edges of locomoting *Dictyostelium* amoebae. *Nature* 341:328–331.
- Futrelle, R.P., Traut, J., and McKee, W.G. (1982): Cell behavior in *Dictyostelium discoideum*: Preaggregation response to localized cyclic AMP pulses. *J. Cell Biol.* 92:807–821.
- Geiger, B., Avnur, Z., Kreis, T.E., and Schlessinger, J. (1984): The dynamics of cytoskeletal organization in areas of cell contact. *Cell Muscle Motil.* 5:195–234.
- Gerisch, G. (1976): Extracellular cyclic-AMP phosphodiesterase regulation in agar plate cultures of *Dictyostelium discoideum*. *Cell Diff.* 5:21–25.
- Gerisch, G. (1979): Control circuits in cell aggregation and differentiation of *Dictyostelium discoideum*. In Ebert, J.D., and Okada, T. (eds.): “Mechanisms of Cell Change.” New York: John Wiley & Sons, pp. 225–239.
- Gerisch, G. (1982): Chemotaxis in *Dictyostelium*. *Annu. Rev. Physiol.* 44:535–552.
- Gerisch, G. (1987): Cyclic AMP and other signals controlling cell development and differentiation in *Dictyostelium*. *Ann. Rev. Biochem.* 56:853–879.
- Gerisch, G., and Malchow, D. (1976): Cyclic AMP receptors and the control of cell aggregation in *Dictyostelium*. *Adv. Cyt. Nuc. Res.* 7:49–68.
- Gerisch, G., and Wick, U. (1975): Intracellular oscillations and release of cyclic AMP from *Dictyostelium* cells. *Biochem. Biophys. Res. Comm.* 65:364–370.
- Gerisch, G., Hülser, D., Malchow, D., and Wick, U. (1975): Cell communication by periodic cyclic-AMP pulses. *Phil. Trans. R. Soc. Lond. B.* 272:181–192.
- Gerisch, G., Malchow, D., Roos, W., and Wick, U. (1979): Oscillations of cyclic nucleotide concentrations in relation to the excitability of *Dictyostelium* cells. *J. Exp. Biol.* 81:33–47.
- Grebecki, A. (1984): Relative motion in *Amoeba proteus* in respect to the adhesion sites. I. Behavior of monotactic forms and the mechanism of fountain phenomenon. *Protoplasma* 123:116–134.
- Grebecki, A. (1986): Adhesion-dependent movements of the cytoskeletal cylinder of amoebae. *Acta Protozool.* 25:255–268.
- Grebecki, A. (1994): Membrane and cytoskeleton flow in motile cells with emphasis on the contribution of free-living amoebae. *Int. Rev. Cyt.* 148:37–80.
- Hammer, J.A., III. (1991): Novel myosins. *Trends Cell Biol.* 1:50–56.
- Hartmann, M. (1953): Eine Einführung in die Lehre vom Leben. In Bauer, H. (ed.): “Allgemeine Biologie.” Stuttgart: Gustav Fischer Verlag, pp. 117–130.
- Hyman, L.H. (1917): Metabolic gradients in amoeba and their relation to the mechanism of amoeboid movement. *J. Exp. Zool.* 24:55–99.
- Inoué, S. (1986): “Video Microscopy.” New York: Plenum Press, pp. 1–584.
- Inoué, S. (1988): Progress in video microscopy. *Cell Motil. Cytoskel.* 10:13–17.
- Inoué, S., and Fukui, Y. (1995): Eupodium: A new cortical structure in *Dictyostelium* amoeba and its dynamics as demonstrated by video DIC microscopy and microbeam release of caged cyclic-AMP. *Mol. Biol. Cell* 6:261a.
- Jung, G., Fukui, Y., Martin, B., and Hammer, J.A., III (1993): Sequence, expression pattern, intracellular localization and targeted disruption of the *Dictyostelium* myosin ID heavy chain isoform. *J. Biol. Chem.* 268:14981–14990.

- Klein P.S., Sun, T.J., Saxe, C.L. III, Kimmel, A.R., Johnson, R.L., and Devereotes, P.N. (1988): A chemoattractant receptor controls development in *Dictyostelium discoideum*. *Science* 241:1467–1472.
- Kolega, J., Shure, M.S., Chen, W.-T., and Young, N.D. (1982): Rapid cellular translocation is related to close contacts formed between various cultured cells and their substrata. *J. Cell Sci.* 54:23–34.
- Konijn, T.M., Chang, Y.Y., and Bonner, J.T. (1969): Synthesis of cyclic AMP in *Dictyostelium discoideum* and *Polysphondylium pallidum*. *Nature* 224:1211–1212.
- Korn, E.D. (1982): Actin polymerization and its regulation by proteins from nonmuscle cells. *Physiol. Rev.* 62:672–737.
- Kreitmeier, M., Gerisch, G., Heizer, C., and Müller-Taubenberger, A. (1995): A talin homologue of *Dictyostelium* rapidly assembles at the leading edge of cells in response to chemoattractant. *J. Cell Biol.* 129:179–188.
- Lakkakorpi, P.T., and Väänänen, H.K. (1991): Kinetics of the osteoclast cytoskeleton during resorption cycle in vitro. *J. Bone and Mineral Res.* 6:817–826.
- Mast, S.O. (1923): Mechanism of locomotion in amoeba. *Proc. Natl. Acad. Sci. USA.* 7:258–261.
- Mast, S.O. (1926): Structure, movement, locomotion, and stimulation in amoeba. *J. Morpho. Physiol.* 41:347–425.
- Matsudaira, P.T., and Burgess, D.R. (1979): Identification and organization of the components in the isolated microvillus cytoskeleton. *J. Cell Biol.* 83:667–673.
- McRobbie, S.J., and Newell, P.C. (1984): Chemoattractant-mediated changes in cytoskeletal actin of cellular slime moulds. *J. Cell Sci.* 68:139–151.
- Mooseker, M.S., Conzelman, K.A., Coleman, T.R., Heuser, J.E., and Sheetz, M.P. (1989): Characterization of intestinal microvillar membrane disks: Detergent-resistant membrane sheets enriched in associated brush border myosin I (110-calmodulin). *J. Cell Biol.* 109:1153–1161.
- Morita, Y., Jung, G., Hammer, J.A. III, and Fukui, Y. (1996): Localization of *Dictyostelium* myosins IB and ID using isoform-specific antibodies. *Eur. J. Cell Biol.* 71:371–379.
- Mueller, S.C., Yeh, Y., and Chen, W.-T. (1992): Tyrosine phosphorylation of membrane proteins mediates cellular invasion by transformed cells. *J. Cell Biol.* 119:1309–1325.
- Nerbonne, J.M., Richard, S., Nargeot, J., and Lester, H.A. (1984): New photoactivatable cyclic nucleotides produce intracellular jumps in cyclic AMP and cyclic GMP concentrations. *Nature* 310:74–76.
- Nermut, M.V., Eason, P., Hirst, E.M.A., and Kellie, S. (1991): Cell/substrate adhesions in RSV-transformed rat fibroblasts. *Exp. Cell Res.* 193:382–397.
- Oster, G. (1988): Biophysics of the leading lamella. *Cell Motil. Cytoskel.* 10:164–171.
- Pantin, C.F.A. (1923): On the physiology of amoeboid movement. *I. J. Martine Biol. Assoc.* 13:24–69.
- Pollard, T.D., Doberstein, S.K., and Zot, H.G. (1991): Myosin-I. *Annu. Rev. Physiol.* 53:653–681.
- Roos, W., Nanjundiah, V., Malchow, D., and Gerisch, G. (1975): Amplification of cyclic-AMP signals in aggregating cells of *Dictyostelium discoideum*. *Fed. Eur. Biochem. Soc. Lett.* 53:139–142.
- Schleicher, M., and Noegel, A.A. (1992): Dynamics of the *Dictyostelium* cytoskeleton during chemotaxis. *The New Biologist*, 4:461–472.
- Schleicher, M., Noegel, A., Schwarz, T., Wallraff, E., Brink, M., Faix, J., Gerisch, G., and Isenberg, G. (1988): A *Dictyostelium* mutant with severe defects in α -actinin: Its characterization using cDNA probes and monoclonal antibodies. *J. Cell Sci.* 90:59–71.
- Sheetz, M.P., Wayne, D.B., and Pearlman, A.L. (1992): Extension of filopodia by motor-dependent actin assembly. *Cell Motil. Cytoskel.* 22:160–169.
- Soll, D.R. (1988): “DMS,” a computer-assisted system for quantitating motility, the dynamics of cytoplasmic flow, and pseudopod formation: Its application to *Dictyostelium* chemotaxis. *Cell Motil. Cytoskel.* 10:91–106.
- Stickel, S.K., and Wang, Y.-L. (1987): Alpha-actinin-containing aggregates in transformed cells are highly dynamic structures. *J. Cell Biol.* 104:1521–1526.
- Swanson, J.A., and Taylor, D.L. (1982): Local and spatially coordinated movements in *Dictyostelium discoideum* amoebae during chemotaxis. *Cell* 28:225–232.
- Tarone, G., Cirillo, D., Giancotti, F.G., Comoglio, P.M., and Marchisio, P.C. (1985): Rous sarcoma virus-transformed fibroblasts adhere primarily at discrete protrusions of the ventral membrane called podosomes. *Exp. Cell Res.* 159:141–157.
- Taylor, D.L., Condeelis, J.S., Moore, P.L., and Allen, R.D. (1973): The contractile basis of amoeboid movement. I. The chemical control of motility in isolated cytoplasm. *J. Cell Biol.* 59:378–394.
- Tilney, L.G., and Inoué, S. (1985): Acrosomal reaction of *Thyone* sperm. III. The relationship between actin assembly and water influx during the extension of the acrosomal process. *J. Cell Biol.* 100:1273–1283.
- Titus, M.A., Kuspa, A., and Loomis, W.F. (1994): Discovery of myosin genes by physical mapping in *Dictyostelium*. *Proc. Natl. Acad. Sci. USA* 91:9446–9450.
- Turner, C.E., and Burridge, K. (1991): Transmembrane molecular assemblies in cell-extracellular matrix interactions. *Curr. Opin. Cell Biol.* 3:849–853.
- Walker, R.A., Inoué, S., and Salmon, E.D. (1989): Asymmetric behavior of severed microtubule ends after ultraviolet-microbeam irradiation of individual microtubules in vitro. *J. Cell Biol.* 108:931–937.
- Wick, U., Malcow, D., and Gerisch, G. (1978): Cyclic-AMP stimulated calcium influx into aggregating cells of *Dictyostelium discoideum*. *Cell Biol. Int. Res.* 2:71–79.
- Witke, W., Schleicher, M., and Noegel, A.A. (1992): Redundancy in the microfilament system. *Dictyostelium* cells that lack two F-actin crosslinking proteins show abnormal multicellular development. *Cell* 68:53–62.
- Wolosewick, J.J. (1984): Distribution of actin in migrating leukocytes in vivo. *Cell Tissue Res.* 236:517–525.
- Yumura, S., and Fukui, Y. (1985): Reversible cyclic AMP-dependent change in distribution of myosin thick filaments in *Dictyostelium*. *Nature* 314:194–196.